The EMBO Journal (2012) 31, 457–470 | © 2012 European Molecular Biology Organization | All Rights Reserved 0261-4189/12
www.embojournal.org

THE EMBO JOURNAL

Palmitoylated TMX and calnexin target to the mitochondria-associated membrane

Emily M Lynes[1], Michael Bui[1], Megan C Yap[1], Matthew D Benson[1], Bobbie Schneider[2], Lars Ellgaard[3], Luc G Berthiaume[1] and Thomas Simmen[1,*]

[1]Department of Cell Biology, Faculty of Medicine and Dentistry, University of Alberta, Edmonton, Alberta, Canada, [2]Fred Hutchinson Cancer Research Center, Electron Microscopy Facility, Seattle, WA, USA and [3]Department of Biology, University of Copenhagen, Copenhagen N, Denmark

The mitochondria-associated membrane (MAM) is a domain of the endoplasmic reticulum (ER) that mediates the exchange of ions, lipids and metabolites between the ER and mitochondria. ER chaperones and oxidoreductases are critical components of the MAM. However, the localization motifs and mechanisms for most MAM proteins have remained elusive. Using two highly related ER oxidoreductases as a model system, we now show that palmitoylation enriches ER-localized proteins on the MAM. We demonstrate that palmitoylation of cysteine residue(s) adjacent to the membrane-spanning domain promotes MAM enrichment of the transmembrane thioredoxin family protein TMX. In addition to TMX, our results also show that calnexin shuttles between the rough ER and the MAM depending on its palmitoylation status. Mutation of the TMX and calnexin palmitoylation sites and chemical interference with palmitoylation disrupt their MAM enrichment. Since ER-localized heme oxygenase-1, but not cytosolic GRP75 require palmitoylation to reside on the MAM, our findings identify palmitoylation as key for MAM enrichment of ER membrane proteins.

The EMBO Journal (2012) **31,** 457–470. doi:10.1038/emboj.2011.384; Published online 1 November 2011
Subject Categories: membranes & transport; signal transduction
Keywords: calnexin; endoplasmic reticulum; mitochondria-associated membrane; palmitoylation; TMX

Introduction

The endoplasmic reticulum (ER) is the point of origin for protein secretion, but is also a critical decision maker for apoptosis. Because of its multiple functions that need to be spatially separated, the ER is a complex assembly of numerous membrane domains, which all show very distinct protein composition (Levine and Rabouille, 2005). Each ER membrane domain is associated with the individual, numerous functions of the ER, including ER protein export at the ER exit site (ERES; Budnik and Stephens, 2009), ER-associated degradation and quality control occurring within the ER quality control compartment (Kamhi-Nesher *et al*, 2001; Lederkremer, 2009), and ER–mitochondria calcium and lipid exchange at the mitochondria-associated membrane (MAM; Hayashi *et al*, 2009; de Brito and Scorrano, 2010). The specific protein composition of these ER domains suggests the existence of intra-ER localization mechanisms that go far beyond the well-known distinction between rough and smooth ER (sER) (Lynes and Simmen, 2011). Contrary to ER retention that is known to depend on the recognition of luminal and cytosolic motifs by the KDEL receptor (Capitani and Sallese, 2009) and the cytosolic COPI coat complex (Murshid and Presley, 2004) as well as the ER redox state (Anelli *et al*, 2003), localization mechanisms to individual domains of the ER are less well understood. It has been hypothesized that rough ER (rER) and sER proteins are able to accumulate within their respective domains depending on the curvature of sheet-like or tubular ER structures (Shibata *et al*, 2010). In the case of the transitional ER (tER), the interaction with components of the COPII coat, a mediator of ER vesicle budding and ER–Golgi transport, serves to target human Sec16 proteins to ERES (Bhattacharyya and Glick, 2007; Hughes *et al*, 2009). Likewise, translocons containing Sec61 proteins serve as a scaffold for oligosaccharyltransferase complexes, but also anchor ribosomes to the rER (Kalies *et al*, 1994; Chavan *et al*, 2005).

Of all the domains of the ER, the MAM has recently received particular attention because of its important roles in lipid and calcium metabolism (de Brito and Scorrano, 2010). This specialized sER membrane domain forms close contacts with the mitochondria and mediates the transfer of newly synthesized lipids and calcium signals from the ER to the mitochondria (Vance, 2003; Hayashi *et al*, 2009). While the anchoring of the ER to mitochondria requires cytosolic and mitochondrial proteins, such as the ERMES complex, mitofusin-2 and GRP75 (Szabadkai *et al*, 2006; de Brito and Scorrano, 2008; Kornmann *et al*, 2009), a diverse group of ER proteins target to the MAM. This group comprises the lipid transfer proteins acyl-coenzyme A:cholesterol acyltransferase/sterol *O*-acyltransferase 1 (ACAT1/SOAT1; Rusinol *et al*, 1994) and diacylglycerol *O*-acyltransferase 2 (DGAT2; Stone *et al*, 2009), lipid synthesizing proteins such as phosphatidylserine synthases 1 and 2 (PSS1 and PSS2; Stone and Vance, 2000), presenilins (Area-Gomez *et al*, 2009), and ER chaperones and oxidoreductases such as calnexin (Myhill *et al*, 2008; Stone *et al*, 2009) and Ero1α (Gilady *et al*, 2010) that interact with sarco/ER Ca^{2+}-ATPase (SERCA) and the inositol 1,4,5-trisphosphate receptor (IP3R), respectively (Roderick *et al*, 2000; Li *et al*, 2009; Anelli *et al*, 2011).

Targeting to the MAM can depend on the presence of a cryptic mitochondrial targeting sequence, as detected within the cytosolic domain of the transmembrane protein DGAT2, but such a motif is absent from other MAM proteins

*Corresponding author. Department of Cell Biology, Faculty of Medicine and Dentistry, University of Alberta, Medical Sciences Building, Room 5-65, Edmonton, Alberta, Canada T6G 2H7. Tel.: +1 780 492 1546; Fax: +1 780 492 0450; E-mail: Thomas.Simmen@ualberta.ca

Received: 22 March 2011; accepted: 27 September 2011; published online: 1 November 2011

(Stone *et al*, 2009). Interestingly, MAM localization is lost for a subset of ER proteins when oxidizing conditions within the ER are disrupted, as observed with Ero1α (Gilady *et al*, 2010), or when cholesterol is depleted from the ER, as observed with the sigma-1 receptor, a regulatory protein for the IP3R (Hayashi and Su, 2007; Hayashi and Fujimoto, 2010). Our laboratory has demonstrated a role for the cytosolic sorting protein phosphofurin acidic cluster sorting protein 2 (PACS-2) in the enrichment of calnexin to the MAM, but this interaction is likely not sufficient for complete MAM enrichment of calnexin (Myhill *et al*, 2008).

Given the paucity of information on MAM targeting mechanisms, we therefore wanted to investigate further how ER proteins are targeted and retained at that site. Because of the presence of the Ero1α oxidoreductase on the MAM (Gilady *et al*, 2010) and the presence of MAM targeting information in the cytosolic domains of MAM proteins (Myhill *et al*, 2008; Stone *et al*, 2009), we decided to focus on four protein disulphide isomerase (PDI) family members, TMX, TMX2, TMX3, and TMX4 (Ellgaard and Ruddock, 2005; Haugstetter *et al*, 2005; Matsuo *et al*, 2009; Roth *et al*, 2009). TMX transmembrane proteins exhibit a cytosolic domain, which could contain targeting information. Among the TMX family members, TMX and TMX4 are most highly related, since they exhibit an overall similar build and 53% identity in their luminal thioredoxin domains (Figure 1A). In the present study, we now show that TMX and TMX2, but not TMX3 and TMX4 are enriched on the MAM. Targeting TMX to the MAM requires palmitoylation of two membrane-proximal cytosolic cysteines, a mechanism recapitulated in the ER chaperone calnexin. Moreover, we also show that mouse heme oxygenase-1 targets to the MAM dependent on palmitoylation. Therefore, palmitoylation of membrane-proximal, cytosolically exposed cysteines is a new MAM sorting signal for ER membrane proteins.

Results

TMX is enriched on the MAM, but not the highly related TMX4

To discover novel intra-ER targeting mechanisms, we examined how a subgroup of transmembrane thioredoxin-related oxidoreductases targets to the domains of the ER (Ellgaard and Ruddock, 2005; Appenzeller-Herzog and Ellgaard, 2008). We first determined which cell line(s) would be suitable for our experiments by analysing the expression levels of TMX, TMX2, TMX3, and TMX4 in HeLa, A375P, Jurkat, Caco2, and M2 melanoma cells (Figure 1A and B; Supplementary Figure S1). This showed that in this selection, TMX4 was only expressed in high amounts in A375P cells, as previously reported (Roth *et al*, 2009). Conversely, HeLa cells expressed high amounts of TMX, TMX2, and TMX3 (Figure 1B). We chose to examine the intra-ER localization of TMX, TMX2, TMX3, and TMX4 by Optiprep gradients of HeLa, Caco2, and A375P cell homogenates. This protocol can reliably discern enrichment of ER proteins to the tER and rER from enrichment on the MAM (Myhill *et al*, 2008; Roth *et al*, 2009; Gilady *et al*, 2010). Consistent with our previously published results, we find markers of the HeLa rER in the middle of the gradient (ERp57, Ribophorin-1), whereas MAM markers migrate at the bottom (ACAT, calnexin), where we also find mitochondria (Supplementary Figure S2). Our results show that TMX and TMX2 were consistently enriched on Optiprep fractions that contain the MAM (Figure 1C; Supplementary Figure S3). In contrast, TMX4 was found in all ER fractions, whereas TMX3 showed a variable distribution, depending on the cell line. Specifically, TMX was found at close to 60% on MAM membranes, compared with only 25% of the TMX4 signal that peaked in rER fractions (Figure 1D). This finding is particularly remarkable, since TMX and TMX4 show high sequence conservation, in particular in the luminal thioredoxin domains that are 53% identical (Roth *et al*, 2009).

To confirm the MAM association of TMX, we analysed its targeting with a Percoll gradient protocol. This showed that TMX is present on MAMs like Ero1α and calnexin, two chaperones that we had previously found enriched on the MAM (Figure 1E; Supplementary Figure S4). Next, we further examined the intracellular distribution of endogenous TMX and TMX4 by immunofluorescence studies using mitotracker to assay for proximity of the oxidoreductases' signals with mitochondria. Consistent with our biochemical assays, the staining pattern of TMX, but not of TMX4 showed considerable overlap with mitotracker and with calnexin, another MAM-enriched ER protein in HeLa cells (Figure 2A and B; Supplementary Figure S5A). While both TMX and TMX4 showed a dispersed reticular staining pattern, closer inspection revealed only a limited overlap of their staining patterns in A375P cells that express both oxidoreductases (Supplementary Figure S5B). These differences were reflected in a Manders coefficient of close to 0.6 for the TMX to mitochondria apposition, but only 0.4 in the case of TMX4 (Figure 2C).

To complete our quantitative assessment of the apposition of TMX and TMX4 with mitochondria, we analysed their distribution in HeLa (TMX) and A375P (TMX, TMX4) cells by immunoelectron microscopy. We frequently detected immunogold particles directed against TMX on membrane tubules in the proximity of mitochondria (Figure 2D and E). However, this was not the case for TMX4 (Figure 2D and F). To exclude a cell line-specific effect, we also examined the distribution of TMX and TMX4 together in A375P cells. Here, we again found that TMX, but not TMX4 was frequently associated with mitochondria (Figure 2D; Supplementary Figure S6). Quantification revealed that in HeLa and A375P cells, 55% of TMX-directed immunogold particles were found close to mitochondria (<100 nm), whereas we could only find 17% of all anti-TMX4 particles in that range of proximity. Instead, many anti-TMX4 immunogold particles were found associated with or in proximity to ribosome-coated tubules that correspond to the rER. Together, our results derived from biochemical analyses, immunofluorescence microscopy and immunoelectron microscopy show conclusively that despite their high degree of homology, TMX primarily targets to the MAM, whereas TMX4 shows no such enrichment and is found throughout the ER.

A combination of the transmembrane and cytosolic domains is necessary and sufficient for the targeting of TMX to the MAM

To identify the sequence and mechanism that are responsible for TMX MAM targeting, we decided to make use of cDNAs for TMX and TMX4 that we had mutagenized to yield luminally tagged versions of the two oxidoreductases with a myc or a FLAG tag right after the ER signal sequence. We were able to reproduce the distribution patterns of

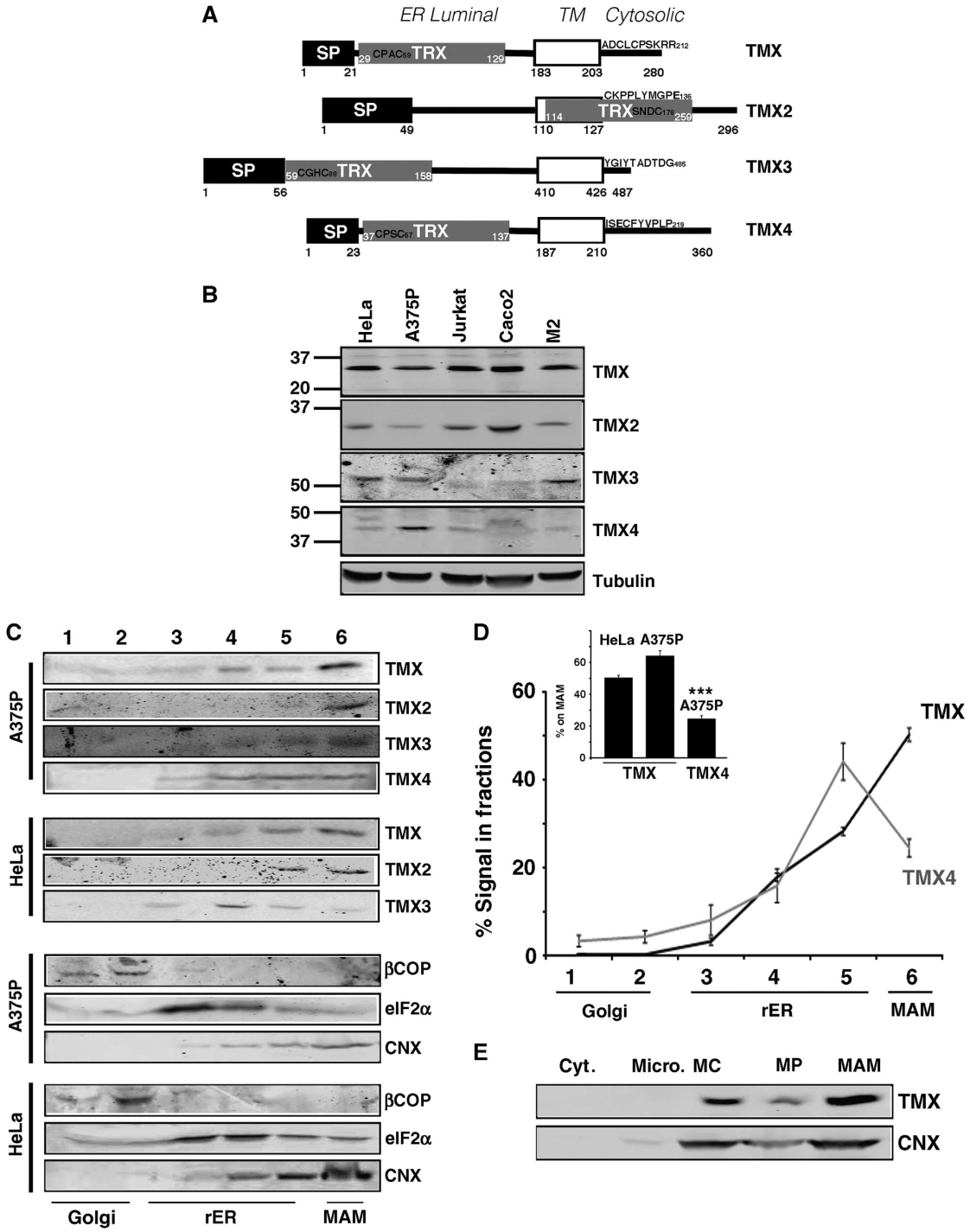

Figure 1 The thioredoxin-related transmembrane protein TMX co-fractionates with the MAM in A375P and HeLa cells. (**A**) Diagram of the topology of TMX proteins. Indicated are signal peptides (SP), thioredoxin domains (TRX), and the transmembrane domains (open boxes). Positions of these domains and of the CXXC active sites are indicated with numbers. (**B**) Analysis of expression levels of TMX family proteins. Lysates from HeLa, A375P, Jurkat, Caco2, and M2 melanoma cells were analysed by western blot for the respective oxidoreductases using α-tubulin as a protein loading control. Molecular weight markers are on the left. (**C**) Analysis of the ER domain distribution of TMX family proteins in A375P and HeLa cells. Cell homogenates were fractionated on an Optiprep gradient. eIF2α indicates the position of the rER (fractions 3–5), βCOP indicates the *cis*-Golgi (fraction 2), the peak of the calnexin signal indicates the MAM (fraction 6). (**D**) Quantification of the fractionation of TMX and TMX4. Three individual experiments in HeLa and A375P cells, respectively, were quantified. The graph shows the distribution of TMX and TMX4 within all fractions, in addition to the respective amounts within fraction 6. (Statistics: $***P = 0.0026$ between HeLa TMX and TMX4, $P = 0.001$ between A375P TMX and TMX4.) (**E**) TMX and calnexin distribution between mitochondria and the MAM. HeLa homogenates were fractionated into cytosol (Cyt.), microsomes (Micro.), crude mitochondria (MC), purified mitochondria (MP), and MAM according to Materials and methods. Equal cell equivalents have been loaded.

endogenous TMX and TMX4 accurately with the myc-tagged (Figure 3A and B) and the FLAG-tagged versions (data not shown). Like endogenous TMX4, myc-tagged TMX4 was not enriched on the MAM, but was distributed fairly evenly to all domains of the ER, as published previously (Figure 3B) (Roth *et al*, 2009) and despite comparable expression levels

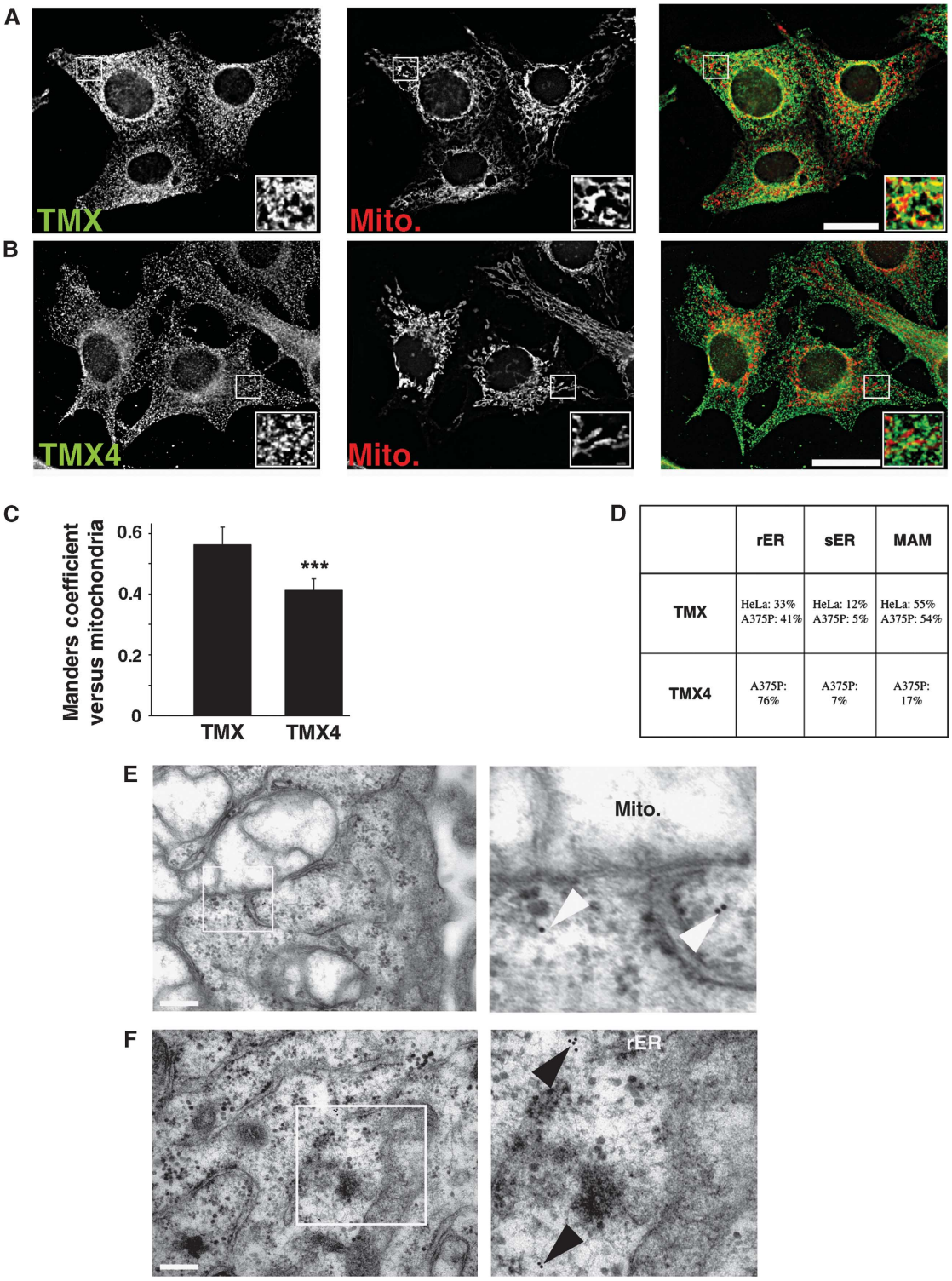

Figure 2 Intracellular localization of endogenous TMX and TMX4. (**A**) HeLa cells were processed for immunofluorescence microscopy for TMX and mitochondria (visualized with Mitotracker). Images were deconvolved. Inserts show a magnified area, indicated with white frames on the bigger pictures. Yellow colour in the overlap indicates apposition of the TMX and mitochondria staining. Scale bar = 25 μm. A representative image is shown. (**B**) A375P cells were processed and imaged as in (**A**) using a mouse TMX4 antibody and mitotracker. (**C**) Quantification of the Manders coefficient for the localization of TMX and TMX4, as shown by representative images in (**A**, **B**). (Statistics: $***P<0.001$.) (**D**) Quantification of TMX and TMX4 immunogold labelling from two independent experiments with the localization of TMX and TMX4 assigned to rER, sER, and MAM (229 particles for TMX in HeLa, 174 particles for TMX4 in A375P). (**E**) HeLa cells were treated for TMX immunogold labelling as described in Materials and methods. A representative image is shown to the left with a zoomed-in area on the right. In all, 10 nm anti-rabbit immunogold particles are highlighted with white arrowheads. Scale bar = 200 nm. (**F**) A375P cells were treated for TMX4 immunogold labelling as described in Materials and methods, a representative image is shown with a zoomed-in area. In all, 10 nm anti-mouse immunogold particles are highlighted with black arrowheads. Scale bar = 200 nm.

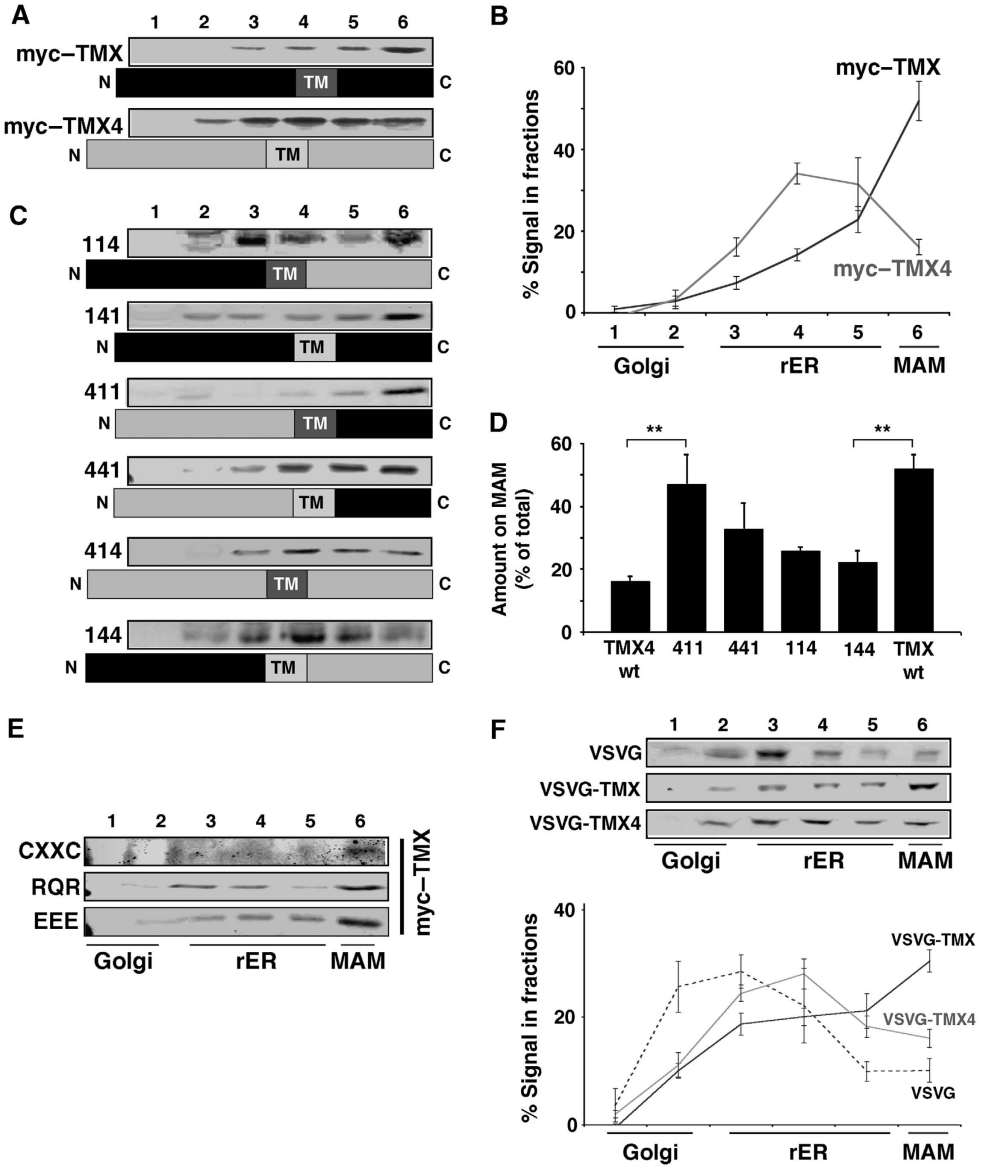

Figure 3 The TMX transmembrane and cytosolic domains are necessary and sufficient for MAM targeting. Except for (**F**), detection of tagged proteins with a polyclonal anti-myc antiserum. (**A**) Optiprep gradient fractionation of luminally myc-tagged TMX and TMX4. HeLa cells transfected with myc–TMX and myc–TMX4 were fractionated on an Optiprep gradient, reproducing the fractionation pattern as seen for endogenous counterparts. (**B**) Quantification of the Optiprep fractionation of myc–TMX and myc–TMX4. Positions of marker proteins are indicated ($n=3$). (**C**) Optiprep gradient analysis of TMX/TMX4 chimera. HeLa cells transfected with TMX/TMX4 chimera were analysed as in (**A**). Chimera has been assigned a code, where 1 stands for TMX and 4 for TMX4 as follows: luminal/transmembrane domain/cytosolic domain. (**D**) Quantification of the Optiprep fractionation for selected TMX/TMX4 chimera. Coding as in (**C**). (Statistics: $^{**}P=0.027$ between TMX4 wt and 411; $P=0.012$ between TMX wt and 144.) (**E**) Optiprep gradient fractionation for selected point mutants. Amino acids indicated stand for alanines that substitute them. CXXC = Δ54–63; RQR = Arg, Glu, Arg267–269 Ala; EEE = Asp248–250 → Ala. (**F**) Optiprep gradient fractionation of VSVG-TMX/TMX4 chimera. HeLa cells transfected with wild-type VSVG and chimera of luminal VSVG fused to transmembrane and cytosolic domains of TMX and TMX4, respectively, were fractionated on an Optiprep gradient. Detection by western blotting with a rabbit anti-VSVG antiserum ($n=3$).

(Supplementary Figure S7). Next, we created luminally tagged chimera of the two proteins. As shown in Figure 3C, we detected the majority of the anti-myc signal in fraction 6 containing the MAM, only when the cytosolic portion of TMX was present (constructs 141, 411, and 441). Of all constructs, the 411 chimera (TMX4 luminal, TMX transmembrane and cytosolic domain) targeted most efficiently to the MAM showing an average enrichment of close to 50% to this membrane domain of the ER on our Optiprep gradient fractionation (Figure 3D). With a candidate approach, we scanned the TMX protein sequence for ER localization signals that could potentially act as MAM retention motifs. This search identified three signals: (i) a CXXC thioredoxin motif in the luminal domain that could connect TMX to ERp44 (Anelli *et al*, 2003); (ii) a RQR C-terminal motif that could localize TMX to the ER and the MAM (Roth *et al*, 2009); and (iii) a cytosolic acidic cluster, which could lead to interaction of TMX with proteins of the PACS family (Youker *et al*, 2009). However, none of these point mutants showed significantly compromised MAM enrichment (Figure 3E).

Thus, we concluded that the combination of the TMX transmembrane and cytosolic domains was most efficient in mediating MAM enrichment and that this combination depended on a hitherto uncharacterized MAM targeting motif.

To test this hypothesis, we fused the TMX transmembrane and cytosolic domains onto the FLAG-tagged luminal domain of vesicular stomatitis virus G (VSVG) protein. Wild-type VSVG protein shows a widespread distribution along the secretory pathway at steady-state conditions (Figure 3F). In contrast, the TMX and TMX4 VSVG chimeric proteins accumulated on the ER. Strikingly, the VSVG-TMX chimera was the only construct that exhibited enrichment on membranes of the MAM (close to 40% of total; Figure 3F). We confirmed these results in fusion proteins with Tac, the IL2 receptor α chain, previously used to examine the contribution of furin and calnexin cytosolic tails to intracellular trafficking (Simmen *et al*, 1999; Okazaki *et al*, 2000) (Supplementary Figure S8). Our results therefore demonstrate that the TMX transmembrane and cytosolic domains contain targeting information that is necessary and sufficient to mediate the enrichment of TMX on the MAM.

Palmitoylation serves as a MAM targeting signal for TMX

When considering additional mechanisms that could lead to the enrichment of TMX on the MAM, we noticed that this oxidoreductase, but also calnexin have both been proposed as palmitoylated proteins (Kang *et al*, 2008; Yount *et al*, 2010; Dowal *et al*, 2011; Forrester *et al*, 2011). Thus, we generated a variant of TMX, in which we mutated the potential palmitoylation sites, two cysteines in a juxtamembrane position (Cys205 and Cys207), into alanines. We transfected this mutant (Myc–TMX CCAA) into HeLa cells and analysed its distribution on the Optiprep gradient. The abrogation of the dual palmitoylation sequence shifted this construct to fractions of the rER and reduced the amount of TMX found in the MAM fraction from $>50\%$ to $<20\%$, when compared with the wild-type protein (Figure 4A). We also transfected FLAG-tagged TMX and TMX4 constructs into HeLa cells and determined their apposition with mitochondria by immunofluorescence. With this approach, we detected significantly lower mitochondrial overlap with TMX CCAA and TMX4, when compared with TMX (Figure 4B and C). Our results suggested that the mutation of the two membrane-proximal cysteines abrogated TMX palmitoylation and its correct intra-ER sorting. To investigate this, we visualized the incorporation of an alkynyl-palmitate analogue into TMX and TMX4 constructs by click chemistry (Kostiuk *et al*, 2009; Yap *et al*, 2010). With this assay, we indeed saw that wild-type TMX, but not the TMX CCAA mutant was readily palmitoylated (Figure 4D). Consistent with a role of palmitoylation in MAM retention, we detected significantly lower levels of palmitoylation on FLAG–TMX4 (Figure 4D). When analysing TMX/TMX4 chimera, where we had replaced the TMX luminal domain with the one of TMX4, we determined that the TMX cytosolic domain provided a substrate for palmitoylation regardless of the presence of the TMX or TMX4 transmembrane domain (Figure 4E). This was also the case when we mutated irrelevant TMX targeting motifs (Supplementary Figure S9).

Since MAM-associated proteins have been found associated with ER-localized Triton-X-114 detergent-resistant membranes (DRMs) (Hayashi and Fujimoto, 2010), we tested whether wild-type TMX and the TMX palmitoylation mutant could be enriched in DRMs. We found that endogenous TMX, FLAG-tagged transfected TMX, but not the TMX palmitoylation mutant (CCAA) target to heavy membrane DRMs (Figure 4F). Neither the luminal protein ERp57 nor the transmembrane oxidoreductase QSOX1 (Coppock and Thorpe, 2006) showed specific targeting to DRMs.

To further test the involvement of palmitoylation in the enrichment of TMX on the MAM, we inhibited palmitoylation in our HeLa cells by the addition of 100 μM 2-bromopalmitate, a known palmitoyl-transferase inhibitor (Yap *et al*, 2010). This reduced the enrichment of endogenous TMX on the MAM (Figure 5A), suggesting that abrogating palmitoylation also abrogates MAM targeting of TMX. We verified that the 2-bromopalmitate did not affect membrane integrity by analysing the distribution of the luminal ER marker PDI and mitochondrial complex 2, as well as the ER-transmembrane calcium handling proteins IP3R type 3 and SERCA2b using our Optiprep fractionation protocol. The MAM amounts of these marker proteins were not reduced by the treatment of HeLa cells with 2-bromopalmitate, but only led to an increased MAM enrichment of SERCA2b (Figure 5A). As an extension of our biochemical studies, we observed that the mitochondria apposition of TMX decreased in the presence of 2-bromopalmitate (Figure 5B and C). Together, these results confirmed that palmitoylation of the juxtamembrane cysteine residues of TMX leads to the enrichment of this oxidoreductase on the MAM and its association with DRMs.

Palmitoylation also directs calnexin to the MAM

In order to determine whether palmitoylation uniquely targets TMX to the MAM, we decided to examine the lectin chaperone calnexin, which we and others had identified earlier as a MAM-enriched ER protein (Hayashi and Su, 2007; Myhill *et al*, 2008; Wieckowski *et al*, 2009). Two observations supported this decision: (i) calnexin is among the set of proteins identified as being palmitoylated (Kang *et al*, 2008; Yount *et al*, 2010; Dowal *et al*, 2011; Forrester *et al*, 2011). (ii) We had demonstrated earlier that calnexin enrichment on the MAM is only partially dependent on the ER sorting molecule PACS-2 (Myhill *et al*, 2008). As a first test for the hypothesis that calnexin also uses palmitoylation for MAM targeting, we examined and quantified the apposition of calnexin with mitochondria in the presence of 2-bromoplamitate compared with control conditions. Like for TMX, we found a significant reduction of the calnexin/mitochondria overlap in cells treated with 2-bromopalmitate (Figure 5D–F).

We therefore decided to examine the effect of site-directed mutagenesis of the two calnexin cysteines in proximity of its transmembrane domain (Cys503/504 of dog calnexin; Figure 6A). This resulted in the significant reduction of calnexin enrichment on the MAM (Figure 6B), the disappearance of palmitoylated calnexin (Figure 6C) and reduced calnexin apposition with mitochondria (Figure 6D and E). However, the mutation of the calnexin palmitoylation site did not affect calnexin's association with DRMs (Figure 6F) and overall, even wild-type calnexin was not significantly enriched on DRMs (compare Figure 4F with 6F). Consistent with the low amounts of cholesterol within ER membranes (Lange *et al*, 1999), β-methyl cyclodextrin did not cause a significant decrease in MAM-localized calnexin and TMX

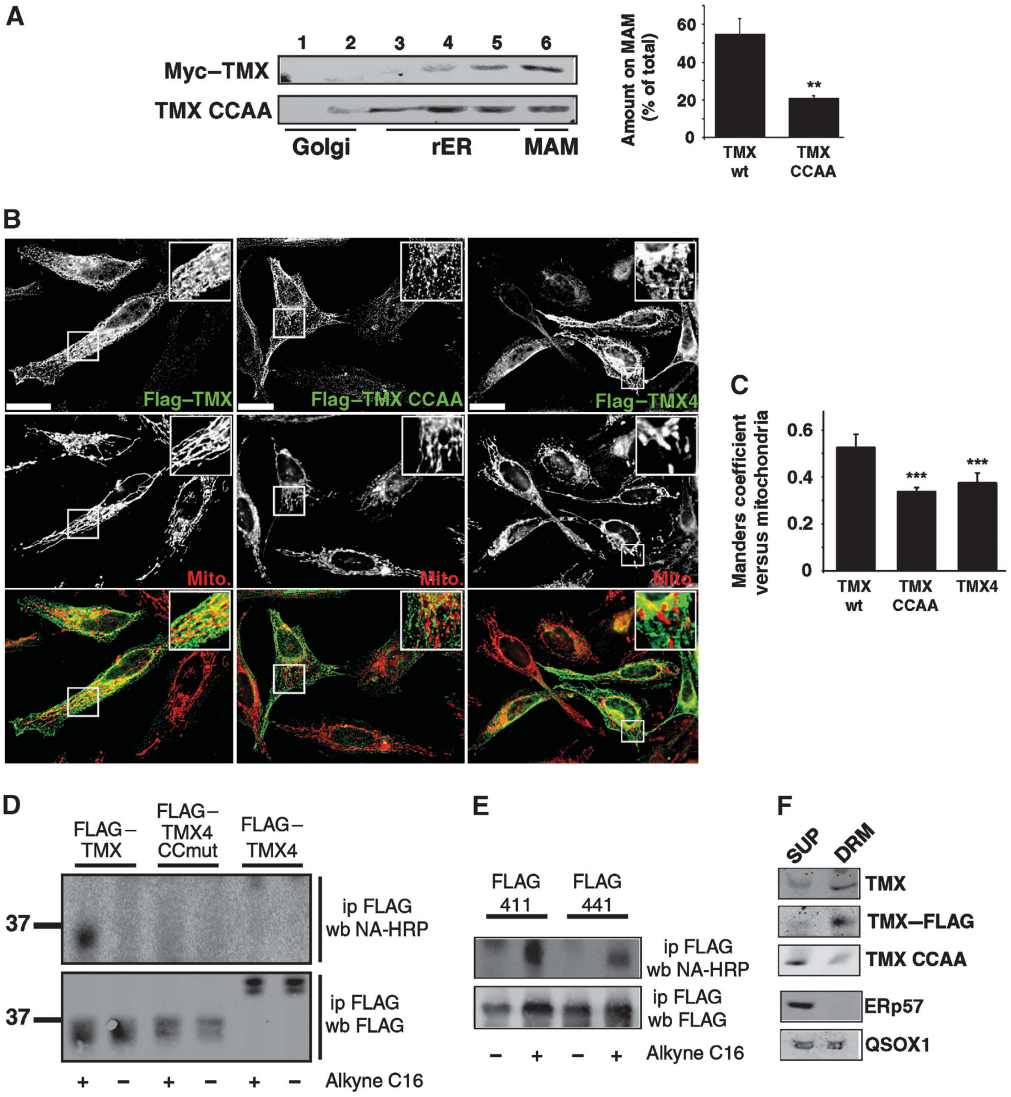

Figure 4 TMX contains two cytosolic, transmembrane-proximal cysteine residues that mediate MAM enrichment. (**A**) Mutagenesis of cysteines 205 and 207 abrogates MAM enrichment of myc-tagged TMX. HeLa cells transfected with myc–TMX and myc–TMX (Cys205, 207→Ala) were fractionated on a discontinuous 10–30% Optiprep gradient, and enrichment of these mutants on the MAM was determined by western blot. A quantification of three independent experiments is shown on the right. (Statistics: $^{**}P = 0.012$ between wt and CCAA TMX.) (**B**) Immunofluorescence localization of FLAG-tagged TMX, TMX CCAA, and TMX4. HeLa cells were transfected for 8 h with the indicated constructs and processed for immunofluorescence microscopy for the FLAG tag and mitochondria (visualized with Mitotracker). Images were deconvolved. Inserts show a magnified area, indicated with white frames on the bigger pictures. Yellow colour in the overlap indicates apposition of the TMX and mitochondria staining. Scale bar = 25 μm. Representative images are shown. (**C**) Quantification of the Manders coefficient for the localization of the constructs, as shown by representative images in (**E**). (Statistics: $^{***}P < 0.001$.) (**D**) Detection of palmitoylation on TMX and TMX4 constructs. Top gel shows the alkynyl-palmitate detection with HRP-conjugated neutravidin. Bottom gel shows the input, as evidenced by the anti-FLAG western blot signal. Size markers are shown on the left. Efficient palmitoylation is detected on FLAG-tagged TMX only. (**E**) Detection of palmitoylation on TMX chimera (labelled as in **C**). Top gel shows the alkynyl-palmitate detection with HRP-conjugated neutravidin. Bottom gel shows the input, as evidenced by the anti-FLAG western blot signal. (**F**) Detection of TMX on DRMs. DRM-associated proteins (DRM) were separated from detergent-soluble supernatants (SUP). Proteins analysed (top to bottom): endogenous TMX, transfected FLAG-tagged TMX, transfected FLAG-tagged TMX CCAA (palmitoylation-deficient mutant). ERp57 and QSOX1 were used as controls.

(Supplementary Figure S10). Moreover, the calnexin transmembrane and cytosolic domains were sufficient to target the VSVG and Tac reporter proteins to the MAM (Figure 6G; Supplementary Figure S8). Therefore, like TMX, calnexin targets to the MAM via its palmitoylation modification.

Palmitoylation of other MAM-associated proteins

Our identification of two ER proteins that use palmitoylation for their MAM enrichment raised the question whether these are an isolated case or part of a larger group of proteins. Given the large number of published palmitoylation proteomes (Kang *et al*, 2008; Yount *et al*, 2010; Dowal *et al*, 2011; Forrester *et al*, 2011), we analysed these lists for the presence of other ER or MAM proteins that could fall within this group. Not considering ER luminal proteins, this analysis led to the identification of mouse heme oxygenase-1, human voltage-dependent anion-selective channel (VDAC) 1 and 2, as well as human GRP75 (also known as HSPA9B). All

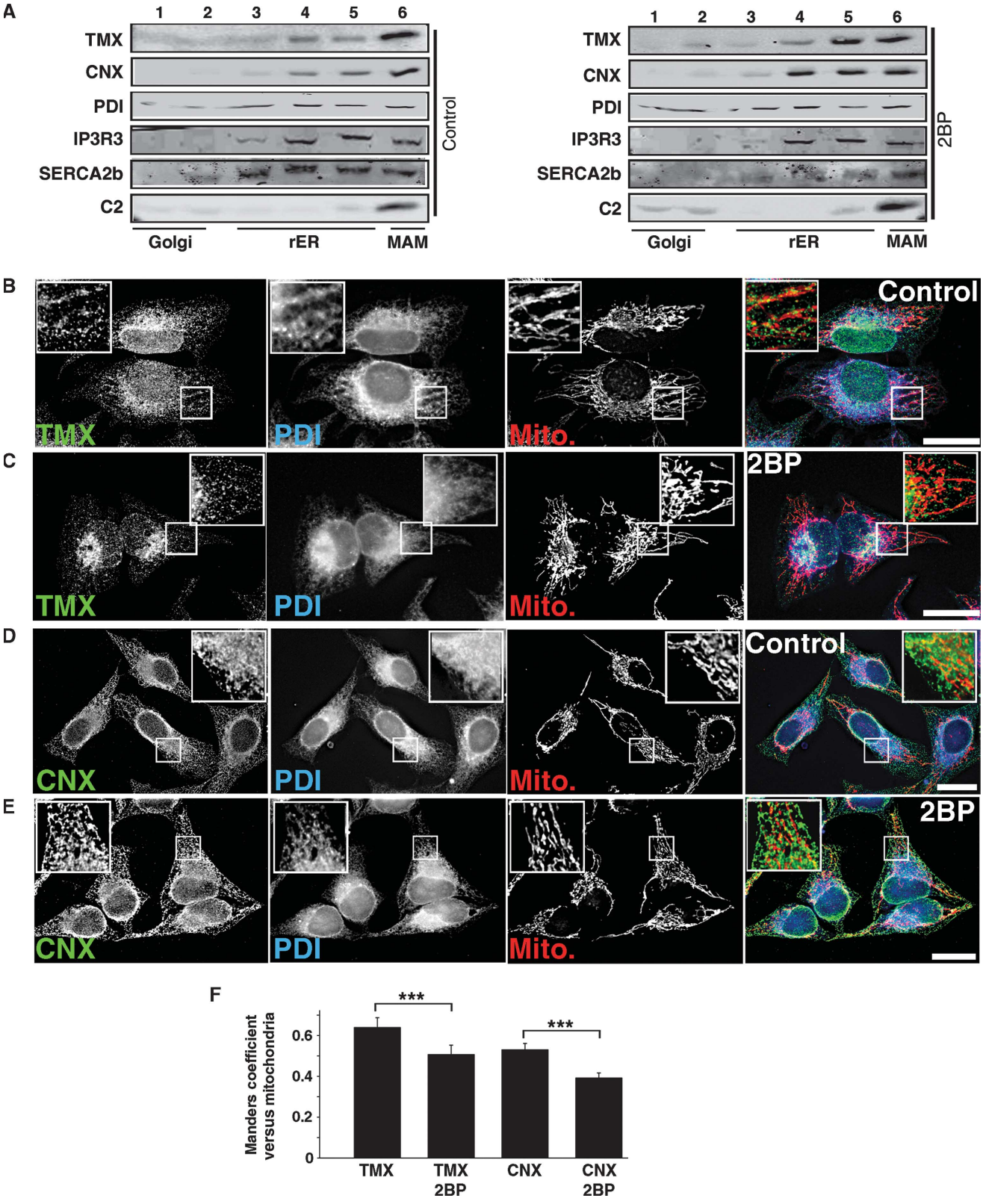

Figure 5 2-Bromopalmitate reduces the apposition of the TMX and calnexin signals with mitochondria. (**A**) Block of palmitoylation with 2-bromopalmitate abrogates MAM enrichment of endogenous TMX and calnexin. HeLa cells were fractionated on an Optiprep gradient, and enrichment of TMX and calnexin on the MAM was determined by western blot. The ER proteins PDI, IP3R3, SERCA2b and the mitochondrial complex 2 serve as controls for MAM integrity. (**B**) HeLa cells were processed for immunofluorescence microscopy for TMX, PDI, and mitochondria (visualized with Mitotracker). Images were deconvolved. Inserts show a magnified area, indicated with white frames on the bigger pictures. Scale bar = 25 μm. A representative image is shown. (**C**) 2-Bromopalmitate-treated HeLa cells were processed for immunofluorescence microscopy as in (**B**). (**D**) HeLa cells were processed for immunofluorescence microscopy for calnexin, PDI, and mitochondria (visualized with Mitotracker). Images were deconvolved. Inserts show a magnified area, indicated with white frames on the bigger pictures. Scale bar = 25 μm. A representative image is shown. (**E**) 2-Bromopalmitate-treated HeLa cells were processed for immunofluorescence microscopy as in (**D**). (**F**) Quantification of the Manders coefficient for the localization of TMX and calnexin, as shown by representative images in (**B**–**E**). (Statistics: ***$P<0.001$ as indicated.)

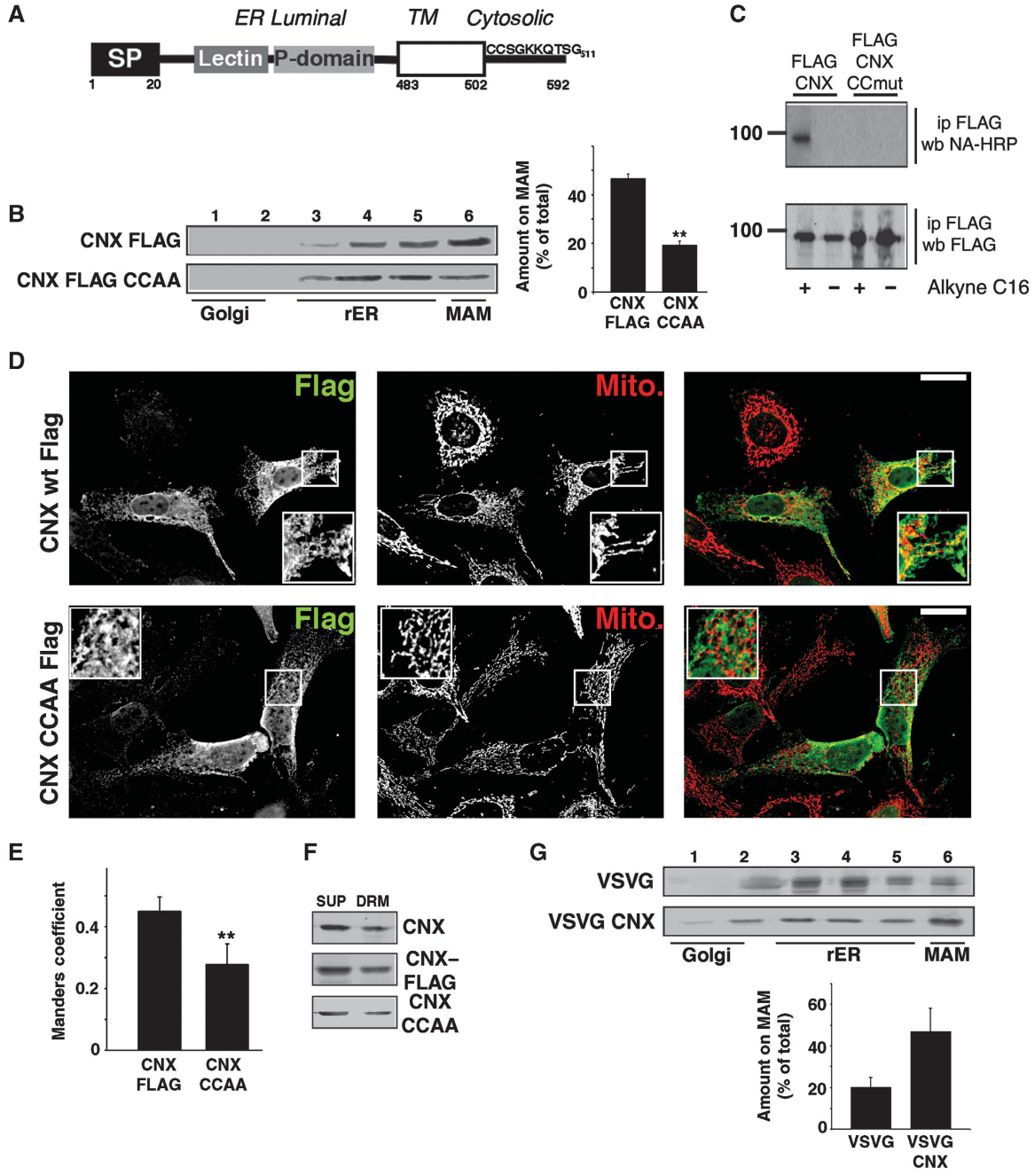

Figure 6 Palmitoylation is necessary and sufficient for calnexin MAM enrichment. (**A**) Diagram of the topology of human calnexin. Indicated are signal peptide (SP), the lectin and P domain, and the transmembrane domain (open box). Positions of selected domains are indicated with numbers. (**B**) Mutagenesis of transmembrane-proximal cysteines 503/504 to alanines abrogates MAM enrichment of FLAG-tagged calnexin. Control HeLa cells and HeLa cells transfected with FLAG–calnexin and FLAG–calnexin (Cys503, 504→Ala) were fractionated on an Optiprep gradient, and enrichment of these proteins on the MAM was determined by western blot. A quantification of three independent experiments is shown on the right. (Statistics: $^{**}P = 0.002$ between CNX wt and CNX CCAA.) (**C**) Detection of palmitoylation on FLAG-tagged calnexin. Top gel shows the alkynyl-palmitate detection with HRP-conjugated neutravidin. Bottom gel shows the input, as evidenced by the anti-FLAG western blotting signal. Size markers are shown on the left. (**D**) Immunofluorescence localization of FLAG-tagged calnexin and calnexin CCAA. HeLa cells were transfected for 8 h with the indicated constructs and processed for immunofluorescence microscopy for the FLAG tag and mitochondria (visualized with Mitotracker). Images were deconvolved. Inserts show a magnified area, indicated with white frames on the bigger pictures. Yellow colour in the overlap indicates apposition of the calnexin and mitochondria staining. Scale bar = 25 μm. Representative images are shown. (**E**) Quantification of the Manders coefficient for the localization of the constructs, as shown by representative images in (**E**). (Statistics: $^{**}P = 0.0044$.) (**F**) Detection of calnexin on DRMs. DRM-associated proteins (DRM) were separated from detergent-soluble supernatants (SUP). Proteins analysed (top to bottom): endogenous calnexin, transfected FLAG-tagged calnexin, transfected FLAG-tagged calnexin CCAA (palmitoylation-deficient mutant). (**G**) Optiprep gradient fractionation of VSVG-calnexin chimera. HeLa cells transfected with wild-type VSVG and chimera of luminal VSVG fused to the transmembrane and cytosolic domain of calnexin were fractionated on an Optiprep gradient. Detection by western blot with a rabbit anti-VSVG antiserum ($n = 3$).

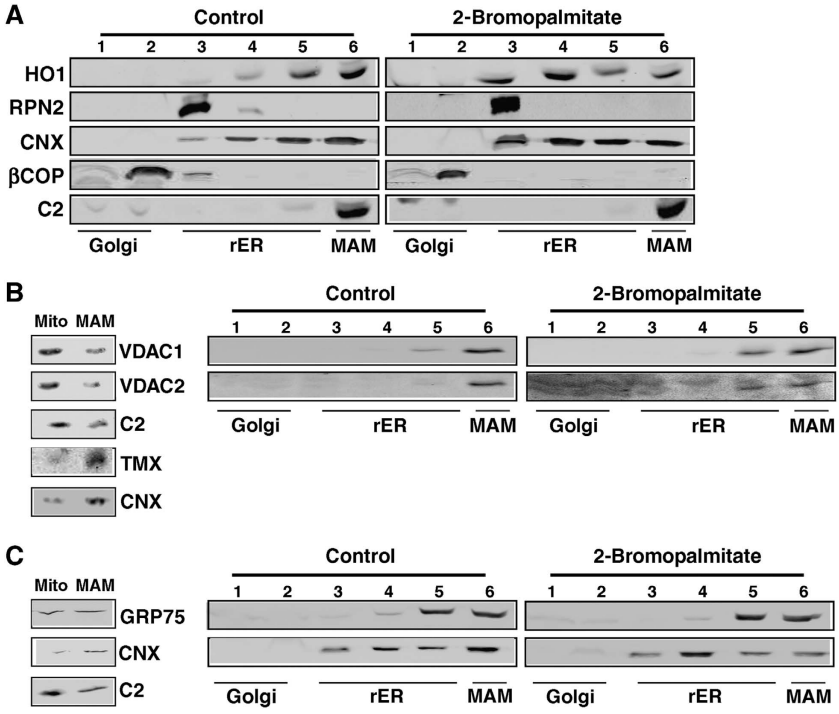

Figure 7 2-Bromopalmitate reduces MAM enrichment of heme oxygenase-1, but not of VDAC1/2 and GRP75. (**A**) Block of palmitoylation with 2-bromopalmitate abrogates MAM enrichment of heme oxygenase-1. B16 cells were fractionated on a discontinuous 10–30% Optiprep gradient, and enrichment of heme oxygenase-1 on the MAM was determined by western blot. The ER proteins ribophorin-2, and calnexin, as well as βCOP and mitochondrial complex 2 serve as controls for MAM integrity. (**B**) VDAC1 and VDAC2 show a 2-bromopalmitate-sensitive moiety. Left gels: Percoll separation of mitochondria and MAM. VDAC1/2 show a mitochondrial distribution, when compared with MAM proteins TMX and calnexin. Right gels: Block of palmitoylation with 2-bromopalmitate shifts a moiety of VDAC1/2 into rER fractions. HeLa cells were fractionated on an Optiprep gradient, and enrichment of VDAC1/2 on the MAM was determined by western blot. (**C**) GRP75 is not mis-localized with 2-bromopalmitate. Left gels: Percoll separation of mitochondria and MAM. GRP75 localizes in part to MAM. Right gels: Block of palmitoylation with 2-bromopalmitate does not affect GRP75. HeLa cells were fractionated on an Optiprep gradient, and enrichment of GRP75 on the MAM was determined by western blot.

proteins in this group could function at the MAM: ER-localized heme oxygenase-1 degrades heme to produce carbon monoxide, an anti-apoptotic molecule that also interferes with cellular ion channels in a mitochondria-dependent manner (Scragg *et al*, 2008; Hwang *et al*, 2009). VDAC family members localize to the outer mitochondrial membrane, but also the ER and are involved in calcium and reactive oxygen species transport (Shoshan-Barmatz and Israelson, 2005; Shoshan-Barmatz and Ben-Hail, 2011). Cytosolic GRP75 bridges the ER to mitochondria by interacting with IP3R and VDAC1 (Szabadkai *et al*, 2006).

We first analysed whether the ER distribution of mouse heme oxygenase-1 was dependent on efficient palmitoylation. This experiment showed that heme oxygenase-1 moved from the MAM fractions to the rER upon a block of palmitoylation (Figure 7A). Next, we tested our hypothesis on human VDAC1 and VDAC2. We detected a small moiety of both proteins on the MAM, but none on other domains of the ER (Figure 7B). Compared with heme oxygenase-1, a much smaller amount of both VDAC proteins moved into the rER upon a block of palmitoylation (Figure 7B). Lastly, we analysed GRP75 in the same way (Figure 7C). Similar to the VDAC proteins, GRP75 did not significantly move to membranes of the rER. Together, our results suggest that palmitoylation of ER membrane, but not of peripheral proteins leads to MAM enrichment.

Discussion

The MAM has emerged as a domain of the ER enriched with numerous, but not all ER chaperones and oxidoreductases (Simmen *et al*, 2010; Lynes and Simmen, 2011). The enrichment of some of these proteins (e.g. calnexin, Ero1α), but not others (e.g. calreticulin, PDI, ERp57) suggests that targeting mechanisms exist for this domain. For example, calnexin targets predominantly to sER domains, contrary to the rER-associated PDI (Iinuma *et al*, 2009), but can redistribute to domains of the rER and the peripheral ER upon activation of Rab32 (Bui *et al*, 2010). Within the sER, calnexin accumulates on the MAM (Myhill *et al*, 2008; Stone *et al*, 2009).

To facilitate the discovery of MAM targeting mechanisms of ER chaperones and oxidoreductases, we chose two highly similar, but differentially localized ER oxidoreductases as a model system: the MAM-enriched TMX and the rER-enriched TMX4 (Figure 1). We demonstrate the MAM enrichment of TMX by four different methods (Optiprep gradient, Percoll gradient, immunofluorescence microscopy, electron microscopy). TMX targets to the MAM using palmitoylation of membrane-proximal cysteines. We were able to identify a similar motif in calnexin as also responsible for MAM enrichment. Our results are summarized in Figure 8, which shows palmitoylated TMX and calnexin enriched on the MAM. Since mutant calnexin and TMX that lack the membrane-proximal cysteines are still retained within the ER, our

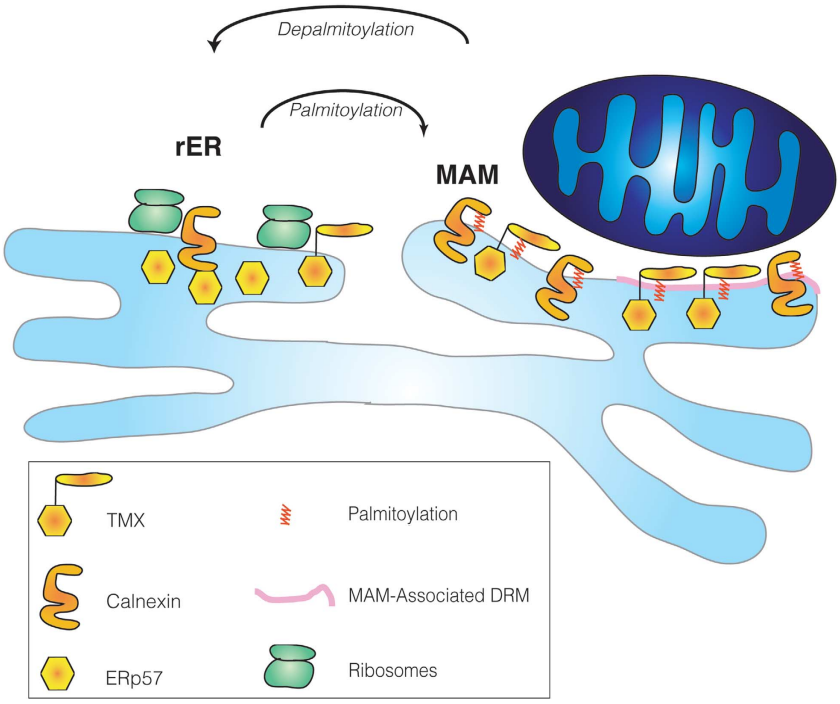

Figure 8 Model for palmitoylation-dependent MAM enrichment of ER chaperones and oxidoreductases. Palmitoylated calnexin and TMX (indicated with the red modifications) target to the MAM, which is composed of DRM (pink domain) and non-DRM.

results also demonstrate that ER domain targeting requires a combination of multiple targeting sequences. In the case of calnexin for example, this includes an acidic cluster in the cytosolic domain that interacts with PACS-2 (Myhill *et al*, 2008); in the case of TMX, this includes a RQR motif similar to TMX4 (Roth *et al*, 2009).

Several recent studies have shown the presence of palmitoylation on several ER and mitochondria proteins, including heme oxygenase-1, reticulon-1, ORAI1, VDAC1, VDAC2, and GRP75 (Kang *et al*, 2008; Yount *et al*, 2010; Dowal *et al*, 2011; Forrester *et al*, 2011). In the present manuscript, we have focused on examining how palmitoylation could mediate their MAM targeting. Indeed, the interference with palmitoylation caused relocation to other ER domains for heme oxygenase-1, but not for VDAC1, VDAC2, and GRP75. Despite this differential response of MAM-localized proteins to a block of palmitoylation, the regulation of palmitoylation should have a big impact on MAM activity and suggests that depalmitoylation could provide an easy mechanism to extract MAM regulatory proteins quickly. Its readout could thus be highly dependent on cell conditions, consistent with opposing observations on 2-bromopalmitate as promoting apoptosis on its own (Cnop *et al*, 2001), but also blocking apoptosis induced by platelet-activating factor (Lu *et al*, 2008).

Palmitoylation of cytosolic cysteine residues is a frequent, post-translational modification that is carried out by a group of protein acyltransferases (PATs) comprising 23 members in mammals, designated as DHHC (Asp–His–His–Cys) PATs (Fukata and Fukata, 2010; Greaves and Chamberlain, 2010). Palmitoylation occurs on cysteine residues of proteins via reversible thioester bonds and this reversibility allows for the regulation of various protein functions including localization to membranes or membrane domains including lipid rafts (Levental *et al*, 2010). At the level of the ER, palmitoylation can promote ER exit of various proteins, including yeast chitin synthase Chs3 and the Wnt signalling protein LRP6 (Lam *et al*, 2006; Abrami *et al*, 2008). However, palmitoylation also blocks lysosomal degradation of ER-localized GluR2 and leads to ER accumulation of ApoB, indicating that ER-associated palmitoylation can have multiple, diverse effects (Zhao *et al*, 2000; Yang *et al*, 2009). This suggests that more than one PAT is associated with the ER. Indeed, 11 PATs have been found at least in part associated with the ER (Ohno *et al*, 2006). Of these, yeast Pfa4p regulates ER exit (Lam *et al*, 2006) and Erf2p promotes plasma membrane localization of Ras (Dong *et al*, 2003), but the functions of most other ER-associated PATs, including all mammalian ER-associated DHHC proteins remain obscure.

One potential mechanism whereby MAM-restricted palmitoylation could affect the localization of transmembrane proteins is by tilting the transmembrane helix to accommodate the membrane width, as shown previously for ER proteins undergoing protein export (Charollais and Van Der Goot, 2009). Along these lines, palmitoylation could accommodate the localization of ER proteins to the MAM by mediating their specific association with DRMs as shown previously for a portion of the sigma-1 receptor (Hayashi and Fujimoto, 2010). Interestingly, numerous additional ER proteins have been found associated with lipid-raft-like domains, including BAP31, erlin-1, and erlin-2 (Browman *et al*, 2006). Indeed, glycosphingolipid-enriched microdomain fractions are found on the MAM (Sano *et al*, 2009). Our results show that TMX not only targets to the MAM, but also efficiently sorts into ER-associated DRMs. However, this is not the case for calnexin, thus raising questions concerning the lipid properties of MAMs.

In summary, using our powerful Optiprep protocol that is able to distinguish between rER and MAM localization, we

have discovered a novel requirement for MAM enrichment that depends on lipid modification. Future research will have to determine regulatory enzymes of this mechanism and the abundance of their target proteins on the MAM.

Materials and methods

Antibodies and reagents

All chemicals were from Sigma (Oakville, ON), except Optiprep (Axis Shield, Norton, MA) and Percoll (GE Healthcare, Baie d'Urfe, QC). The polyclonal antibody against VSVG was a gift from Tom Hobman, Edmonton, AB. The polyclonal antisera against TMX3 and TMX4 (used for western blot) have been described (Haugstetter *et al*, 2005; Roth *et al*, 2009). The mouse monoclonal antiserum against TMX4 (used for immunofluorescence and immunoelectron microscopy) was made by ImmunoKontact/AMS Biotechnology (Abingdon, UK) using a CTAGPEEAALPPEQSRVQ peptide directed against amino acids 24–40, the sequence immediately following the signal peptide (Figure 1A; Supplementary Figure S1). The rabbit anti-calnexin antiserum was generated using a cytosolic peptide by Open Biosystems (Huntsville, AL). Antibodies to TMX (Sigma), PDI, ERp57, GRP75/HSPA9B (Pierce/Fisher, Rockford, IL), heme oxygenase-1, VDAC1, VDAC2 (Abcam, Cambridge, UK), IP3R3 (BD Biosciences, Mississauga, ON), eIF2α (Cell Signaling, Danvers, MA), TMX2 (Lifespan Biosciences, Seattle, WA), βCOP, QSOX1 (Genetex, San Antonio, TX), mitochondrial complex 2 (Mitosciences, Eugene, OR), CD25/Tac (Anaspec, San Jose, CA), SERCA2b, polyclonal and monoclonal anti-Myc (Millipore, Billerica, MA), and the FLAG tag (Rockland, Gilbertsville, PA) were purchased as indicated. HeLa, Jurkat, and Caco2 cells were from ECACC (Porton Down, UK), B16 cells were from A Quest (Santiago, Chile), A375P cells were from E Sviderskaya (London, UK), and M2 melanoma cells were from T Stossel (Boston, MA).

Expression vectors and mutagenesis

FLAG-tagged dog calnexin was previously described (Myhill *et al*, 2008). For heterologous expression, myc- and FLAG-tagged TMX and TMX4 were generated with site-directed mutagenesis on human IMAGE EST clones (Invitrogen, Carlsbad, CA) by inserting the myc- and FLAG-coding sequences after the respective signal peptides. To allow for parallel detection, VSVG-fusion constructs also exhibit a luminal FLAG tag after the VSVG signal peptide. CD25/Tac constructs fuse the calnexin and TMX transmembrane and cytosolic domains to the CD25/Tac luminal portion. All constructs were generated by PCR-based splicing by overlap extension as previously described (Simmen *et al*, 1999). Oligo sequences for all constructs are available upon request. The shTMX GFP construct was from Genecopoiea (Rockville, MD), TMX and TMX4 siRNAs were from Invitrogen.

Optiprep and percoll gradient fractionation

Post-nuclear membranes of HeLa and A375P cells were fractionated on a discontinuous 10–30% Optiprep and Percoll gradient fractionation of MAM and mitochondria was described previously (Gilady *et al*, 2010).

DRM isolation

For the isolation of DRMs, we used a protocol adapted from Hayashi and Fujimoto (2010). In all, $6 \times 10E6$ HeLa cells (transfected as indicated) were lysed in homogenization buffer. The low-speed pellet of post-nuclear membranes was resuspended at 4 °C in 0.5 ml of TNE buffer (10 mM Tris at pH 7.4, 150 mM NaCl, COMPLETE protease inhibitor, 5 mM EDTA). Subsequently, heavy cell membranes were sonicated at 4 °C. To this suspension, 12 μl of a 20% Triton-X-114 solution was added (0.5% final concentration). The suspension was incubated for 30 min at 4 °C and then centrifuged at 100 000 *g* for 1 h in a TLA120.2 rotor. The pellet (DRM fraction) and the supernatant (detergent-soluble fraction) were analysed by western blot.

Immunofluorescence microscopy

Immunofluorescence microscopy images were prepared as described (Gilady *et al*, 2010). Overlap between the ER proteins and the mitochondria, as represented by the Manders coefficient (Manders *et al*, 1996), was determined using Imaris 7.2 software (Bitplane, Zürich, Switzerland) from a minimum of six cells. Images were masked in three dimensions such that the outline of the region of interest closely followed the outline of the cell. A PSF width of 0.218 was determined for the objective lens and used in all calculations. Images were thresholded automatically using the Imaris algorithm, and a Manders coefficient was determined for each image.

Immunoelectron microscopy

HeLa (TMX) and A375P (TMX4) cells on 15-cm dishes were incubated with a 1:1 mix of DMEM/10% fetal bovine serum and fixative (3% paraformaldehyde and 0.2% glutaraldehyde in 0.1 M phosphate buffer, pH 7.4). Cells were then scraped and transferred into an Eppendorf tube and centrifuged at 40 g for 5 min. To fix cells, they were resuspended with 100% fixative and incubated for 4 h at RT. Fixed cells were subsequently processed at the Fred Hutchinson Cancer Research Center (Seattle, WA). Localization of the rabbit anti-TMX antibodies was detected using 10 nm (HeLa) and 15 nm (A375P) gold particles, localization of the mouse anti-TMX4 antibodies was detected using 10-nm gold particles. Quantification was performed on 50 sections each from multiple cells. Assignment to rER (presence of ribosomes) and MAM (proximity <100 nm) was done by visual inspection for a minimum of 100 gold particles from 4 to 8 cells each. Background label on non-identifiable structures (<50% of total label) and labelling within the nucleus (also observed by immunofluorescence; see e.g. Figures 2B and 6C) were not counted.

Detection of palmitoylation using click chemistry

HeLa cells were transfected with FLAG–calnexin, FLAG–TMX, or FLAG–TMX4. After 48 h, cells were labelled with 100 μM alkynyl-palmitate or palmitate conjugated to BSA for 3 h as described in Yap *et al* (2010). Cells were harvested in 0.1% SDS-RIPA buffer (containing CPI protease inhibitor, EDTA-free; Roche, Laval, QC) and calnexin, TMX, and TMX4 proteins were immunoprecipitated using the anti-FLAG antibody (Rockland). The click reaction was then carried out on the immunoprecipitated, labelled proteins by incubating them for 30 min at 37 °C with 2 mM TBTA, 50 mM $CuSO_4$, 50 mM TCEP, and 2 mM Biotin-azide. Samples were then separated in duplicate by SDS–PAGE, and transferred to PVDF membranes, which were washed with either 0.1 M Tris–HCl pH 7.0 or 0.1 M KOH. This alkali treatment removes fatty acids incorporated into proteins via thioester bonds but not via amide bonds and contributes to ensure the specificity of the signal. Palmitoylation was detected by probing both membranes with HRP-conjugated Neutravidin using ECL.

Supplementary data

Supplementary data are available at *The EMBO Journal* Online (http://www.embojournal.org).

Acknowledgements

We thank Elena Posse de Chaves for helpful discussions. Research in the Simmen laboratory was supported by Alberta Cancer Foundation grant #25018, CCSRI Grant 2010-700306 and Alberta Innovates Health Solutions scholarship 200500396. Emily Lynes was supported by Alberta Cancer Foundation studentships 24136 and 25370. The Berthiaume laboratory was supported by Alberta Cancer Foundation Grant #24425. The Ellgaard laboratory was supported by the Novo Nordisk Foundation.

Author contributions: TS designed most of the experiments and performed immunofluorescence microscopy and imaging as well as cDNA cloning; EML and LGB participated in designing the experiments; EML performed most of the experiments and cDNA cloning; MB and MDB assisted with fractionation; MCY performed palmitoylation assays; BS performed electron microscopy; LE provided reagents and edited the manuscript; and EML and TS analysed the data and wrote the manuscript.

Conflict of interest

The authors declare that they have no conflict of interest.

References

Abrami L, Kunz B, Iacovache I, van der Goot FG (2008) Palmitoylation and ubiquitination regulate exit of the Wnt signaling protein LRP6 from the endoplasmic reticulum. *Proc Natl Acad Sci USA* **105:** 5384–5389

Anelli T, Alessio M, Bachi A, Bergamelli L, Bertoli G, Camerini S, Mezghrani A, Ruffato E, Simmen T, Sitia R (2003) Thiol-mediated protein retention in the endoplasmic reticulum: the role of ERp44. *EMBO J* **22:** 5015–5022

Anelli T, Bergamelli L, Margittai E, Rimessi A, Fagioli C, Malgaroli A, Pinton P, Ripamonti M, Rizzuto R, Sitia R (2011) Ero1alpha regulates Ca2+ fluxes at the endoplasmic reticulum-mitochondria interface (MAM). *Antioxid Redox Signal* (in press)

Appenzeller-Herzog C, Ellgaard L (2008) The human PDI family: versatility packed into a single fold. *Biochim Biophys Acta* **1783:** 535–548

Area-Gomez E, de Groof AJ, Boldogh I, Bird TD, Gibson GE, Koehler CM, Yu WH, Duff KE, Yaffe MP, Pon LA, Schon EA (2009) Presenilins are enriched in endoplasmic reticulum membranes associated with mitochondria. *Am J Pathol* **175:** 1810–1816

Bhattacharyya D, Glick BS (2007) Two mammalian Sec16 homologues have nonredundant functions in endoplasmic reticulum (ER) export and transitional ER organization. *Mol Biol Cell* **18:** 839–849

Browman DT, Resek ME, Zajchowski LD, Robbins SM (2006) Erlin-1 and erlin-2 are novel members of the prohibitin family of proteins that define lipid-raft-like domains of the ER. *J Cell Sci* **119:** 3149–3160

Budnik A, Stephens DJ (2009) ER exit sites–localization and control of COPII vesicle formation. *FEBS Lett* **583:** 3796–3803

Bui M, Gilady SY, Fitzsimmons RE, Benson MD, Lynes EM, Gesson K, Alto NM, Strack S, Scott JD, Simmen T (2010) Rab32 modulates apoptosis onset and mitochondria-associated membrane (MAM) properties. *J Biol Chem* **285:** 31590–31602

Capitani M, Sallese M (2009) The KDEL receptor: new functions for an old protein. *FEBS Lett* **583:** 3863–3871

Charollais J, Van Der Goot FG (2009) Palmitoylation of membrane proteins (Review). *Mol Membr Biol* **26:** 55–66

Chavan M, Yan A, Lennarz WJ (2005) Subunits of the translocon interact with components of the oligosaccharyl transferase complex. *J Biol Chem* **280:** 22917–22924

Cnop M, Hannaert JC, Hoorens A, Eizirik DL, Pipeleers DG (2001) Inverse relationship between cytotoxicity of free fatty acids in pancreatic islet cells and cellular triglyceride accumulation. *Diabetes* **50:** 1771–1777

Coppock DL, Thorpe C (2006) Multidomain flavin-dependent sulfhydryl oxidases. *Antioxid Redox Signal* **8:** 300–311

de Brito OM, Scorrano L (2008) Mitofusin 2 tethers endoplasmic reticulum to mitochondria. *Nature* **456:** 605–610

de Brito OM, Scorrano L (2010) An intimate liaison: spatial organization of the endoplasmic reticulum-mitochondria relationship. *EMBO J* **29:** 2715–2723

Dong X, Mitchell DA, Lobo S, Zhao L, Bartels DJ, Deschenes RJ (2003) Palmitoylation and plasma membrane localization of Ras2p by a nonclassical trafficking pathway in Saccharomyces cerevisiae. *Mol Cell Biol* **23:** 6574–6584

Dowal L, Yang W, Freeman MR, Steen H, Flaumenhaft R (2011) Proteomic analysis of palmitoylated platelet proteins. *Blood* **118:** e62–e73

Ellgaard L, Ruddock LW (2005) The human protein disulphide isomerase family: substrate interactions and functional properties. *EMBO Rep* **6:** 28–32

Forrester MT, Hess DT, Thompson JW, Hultman R, Moseley MA, Stamler JS, Casey PJ (2011) Site-specific analysis of protein S-acylation by resin-assisted capture. *J Lipid Res* **52:** 393–398

Fukata Y, Fukata M (2010) Protein palmitoylation in neuronal development and synaptic plasticity. *Nat Rev Neurosci* **11:** 161–175

Gilady SY, Bui M, Lynes EM, Benson MD, Watts R, Vance JE, Simmen T (2010) Ero1alpha requires oxidizing and normoxic conditions to localize to the mitochondria-associated membrane (MAM). *Cell Stress Chaperones* **15:** 619–629

Greaves J, Chamberlain LH (2010) S-acylation by the DHHC protein family. *Biochem Soc Trans* **38:** 522–524

Haugstetter J, Blicher T, Ellgaard L (2005) Identification and characterization of a novel thioredoxin-related transmembrane protein of the endoplasmic reticulum. *J Biol Chem* **280:** 8371–8380

Hayashi T, Fujimoto M (2010) Detergent-resistant microdomains determine the localization of sigma-1 receptors to the endoplasmic reticulum-mitochondria junction. *Mol Pharmacol* **77:** 517–528

Hayashi T, Rizzuto R, Hajnoczky G, Su TP (2009) MAM: more than just a housekeeper. *Trends Cell Biol* **19:** 81–88

Hayashi T, Su TP (2007) Sigma-1 receptor chaperones at the ER-mitochondrion interface regulate Ca(2+) signaling and cell survival. *Cell* **131:** 596–610

Hughes H, Budnik A, Schmidt K, Palmer KJ, Mantell J, Noakes C, Johnson A, Carter DA, Verkade P, Watson P, Stephens DJ (2009) Organisation of human ER-exit sites: requirements for the localisation of Sec16 to transitional ER. *J Cell Sci* **122:** 2924–2934

Hwang HW, Lee JR, Chou KY, Suen CS, Hwang MJ, Chen C, Shieh RC, Chau LY (2009) Oligomerization is crucial for the stability and function of heme oxygenase-1 in the endoplasmic reticulum. *J Biol Chem* **284:** 22672–22679

Iinuma T, Aoki T, Arasaki K, Hirose H, Yamamoto A, Samata R, Hauri HP, Arimitsu N, Tagaya M, Tani K (2009) Role of syntaxin 18 in the organization of endoplasmic reticulum subdomains. *J Cell Sci* **122:** 1680–1690

Kalies KU, Gorlich D, Rapoport TA (1994) Binding of ribosomes to the rough endoplasmic reticulum mediated by the Sec61p-complex. *J Cell Biol* **126:** 925–934

Kamhi-Nesher S, Shenkman M, Tolchinsky S, Fromm SV, Ehrlich R, Lederkremer GZ (2001) A novel quality control compartment derived from the endoplasmic reticulum. *Mol Biol Cell* **12:** 1711–1723

Kang R, Wan J, Arstikaitis P, Takahashi H, Huang K, Bailey AO, Thompson JX, Roth AF, Drisdel RC, Mastro R, Green WN, Yates III JR, Davis NG, El-Husseini A (2008) Neural palmitoyl-proteomics reveals dynamic synaptic palmitoylation. *Nature* **456:** 904–909

Kornmann B, Currie E, Collins SR, Schuldiner M, Nunnari J, Weissman JS, Walter P (2009) An ER-mitochondria tethering complex revealed by a synthetic biology screen. *Science* **325:** 477–481

Kostiuk MA, Keller BO, Berthiaume LG (2009) Non-radioactive detection of palmitoylated mitochondrial proteins using an azido-palmitate analogue. *Methods Enzymol* **457:** 149–165

Lam KK, Davey M, Sun B, Roth AF, Davis NG, Conibear E (2006) Palmitoylation by the DHHC protein Pfa4 regulates the ER exit of Chs3. *J Cell Biol* **174:** 19–25

Lange Y, Ye J, Rigney M, Steck TL (1999) Regulation of endoplasmic reticulum cholesterol by plasma membrane cholesterol. *J Lipid Res* **40:** 2264–2270

Lederkremer GZ (2009) Glycoprotein folding, quality control and ER-associated degradation. *Curr Opin Struct Biol* **19:** 515–523

Levental I, Grzybek M, Simons K (2010) Greasing their way: lipid modifications determine protein association with membrane rafts. *Biochemistry* **49:** 6305–6316

Levine T, Rabouille C (2005) Endoplasmic reticulum: one continuous network compartmentalized by extrinsic cues. *Curr Opin Cell Biol* **17:** 362–368

Li G, Mongillo M, Chin KT, Harding H, Ron D, Marks AR, Tabas I (2009) Role of ERO1-alpha-mediated stimulation of inositol 1,4,5-triphosphate receptor activity in endoplasmic reticulum stress-induced apoptosis. *J Cell Biol* **186:** 783–792

Lu J, Caplan MS, Li D, Jilling T (2008) Polyunsaturated fatty acids block platelet-activating factor-induced phosphatidylinositol 3 kinase/Akt-mediated apoptosis in intestinal epithelial cells. *Am J Physiol Gastrointest Liver Physiol* **294:** G1181–G1190

Lynes EM, Simmen T (2011) Urban planning of the endoplasmic reticulum (ER): How diverse mechanisms segregate the many functions of the ER. *Biochim Biophys Acta* **1813:** 1893–1905

Manders EM, Hoebe R, Strackee J, Vossepoel AM, Aten JA (1996) Largest contour segmentation: a tool for the localization of spots in confocal images. *Cytometry* **23:** 15–21

Matsuo Y, Masutani H, Son A, Kizaka-Kondoh S, Yodoi J (2009) Physical and functional interaction of transmembrane thioredoxin-related protein with major histocompatibility complex class I heavy chain: redox-based protein quality control and its potential relevance to immune responses. *Mol Biol Cell* **20:** 4552–4562

Murshid A, Presley JF (2004) ER-to-Golgi transport and cytoskeletal interactions in animal cells. *Cell Mol Life Sci* **61:** 133–145

Myhill N, Lynes EM, Nanji JA, Blagoveshchenskaya AD, Fei H, Carmine Simmen K, Cooper TJ, Thomas G, Simmen T (2008) The subcellular distribution of calnexin is mediated by PACS-2. *Mol Biol Cell* **19:** 2777–2788

Ohno Y, Kihara A, Sano T, Igarashi Y (2006) Intracellular localization and tissue-specific distribution of human and yeast DHHC cysteine-rich domain-containing proteins. *Biochim Biophys Acta* **1761:** 474–483

Okazaki Y, Ohno H, Takase K, Ochiai T, Saito T (2000) Cell surface expression of calnexin, a molecular chaperone in the endoplasmic reticulum. *J Biol Chem* **275:** 35751–35758

Roderick HL, Lechleiter JD, Camacho P (2000) Cytosolic phosphorylation of calnexin controls intracellular Ca(2+) oscillations via an interaction with SERCA2b. *J Cell Biol* **149:** 1235–1248

Roth D, Lynes E, Riemer J, Hansen HG, Althaus N, Simmen T, Ellgaard L (2009) A di-arginine motif contributes to the ER localization of the type I transmembrane ER oxidoreductase TMX4. *Biochem J* **425:** 195–205

Rusinol AE, Cui Z, Chen MH, Vance JE (1994) A unique mitochondria-associated membrane fraction from rat liver has a high capacity for lipid synthesis and contains pre-Golgi secretory proteins including nascent lipoproteins. *J Biol Chem* **269:** 27494–27502

Sano R, Annunziata I, Patterson A, Moshiach S, Gomero E, Opferman J, Forte M, d'Azzo A (2009) GM1-ganglioside accumulation at the mitochondria-associated ER membranes links ER stress to Ca(2+)-dependent mitochondrial apoptosis. *Mol Cell* **36:** 500–511

Scragg JL, Dallas ML, Wilkinson JA, Varadi G, Peers C (2008) Carbon monoxide inhibits L-type Ca2+ channels via redox modulation of key cysteine residues by mitochondrial reactive oxygen species. *J Biol Chem* **283:** 24412–24419

Shibata Y, Shemesh T, Prinz WA, Palazzo AF, Kozlov MM, Rapoport TA (2010) Mechanisms determining the morphology of the peripheral ER. *Cell* **143:** 774–788

Shoshan-Barmatz V, Ben-Hail D (2011) VDAC, a multi-functional mitochondrial protein as a pharmacological target. *Mitochondrion* (in press)

Shoshan-Barmatz V, Israelson A (2005) The voltage-dependent anion channel in endoplasmic/sarcoplasmic reticulum: characterization, modulation and possible function. *J Membr Biol* **204:** 57–66

Simmen T, Lynes EM, Gesson K, Thomas G (2010) Oxidative protein folding in the endoplasmic reticulum: tight links to the mitochondria-associated membrane (MAM). *Biochim Biophys Acta* **1798:** 1465–1473

Simmen T, Nobile M, Bonifacino JS, Hunziker W (1999) Basolateral sorting of furin in MDCK cells requires a phenylalanine-isoleucine motif together with an acidic amino acid cluster. *Mol Cell Biol* **19:** 3136–3144

Stone SJ, Levin MC, Zhou P, Han J, Walther TC, Farese Jr RV (2009) The endoplasmic reticulum enzyme DGAT2 is found in mitochondria-associated membranes and has a mitochondrial targeting signal that promotes its association with mitochondria. *J Biol Chem* **284:** 5352–5361

Stone SJ, Vance JE (2000) Phosphatidylserine synthase-1 and -2 are localized to mitochondria-associated membranes. *J Biol Chem* **275:** 34534–34540

Szabadkai G, Bianchi K, Varnai P, De Stefani D, Wieckowski MR, Cavagna D, Nagy AI, Balla T, Rizzuto R (2006) Chaperone-mediated coupling of endoplasmic reticulum and mitochondrial Ca2+ channels. *J Cell Biol* **175:** 901–911

Vance JE (2003) Molecular and cell biology of phosphatidylserine and phosphatidylethanolamine metabolism. *Prog Nucleic Acid Res Mol Biol* **75:** 69–111

Wieckowski MR, Giorgi C, Lebiedzinska M, Duszynski J, Pinton P (2009) Isolation of mitochondria-associated membranes and mitochondria from animal tissues and cells. *Nat Protoc* **4:** 1582–1590

Yang G, Xiong W, Kojic L, Cynader MS (2009) Subunit-selective palmitoylation regulates the intracellular trafficking of AMPA receptor. *Eur J Neurosci* **30:** 35–46

Yap MC, Kostiuk MA, Martin DD, Perinpanayagam MA, Hak PG, Siddam A, Majjigapu JR, Rajaiah G, Keller BO, Prescher JA, Wu P, Bertozzi CR, Falck JR, Berthiaume LG (2010) Rapid and selective detection of fatty acylated proteins using omega-alkynyl-fatty acids and click chemistry. *J Lipid Res* **51:** 1566–1580

Youker RT, Shinde U, Day R, Thomas G (2009) At the crossroads of homoeostasis and disease: roles of the PACS proteins in membrane traffic and apoptosis. *Biochem J* **421:** 1–15

Yount JS, Moltedo B, Yang YY, Charron G, Moran TM, Lopez CB, Hang HC (2010) Palmitoylome profiling reveals S-palmitoylation-dependent antiviral activity of IFITM3. *Nat Chem Biol* **6:** 610–614

Zhao Y, McCabe JB, Vance J, Berthiaume LG (2000) Palmitoylation of apolipoprotein B is required for proper intracellular sorting and transport of cholesteroyl esters and triglycerides. *Mol Biol Cell* **11:** 721–734

